



Corrigendum to

“New particle formation from sulfuric acid and ammonia: nucleation and growth model based on thermodynamics derived from CLOUD measurements for a wide range of conditions” published in Atmos. Chem. Phys., 19, 5033–5050, 2019

Andreas Kürten

Institute for Atmospheric and Environmental Sciences, Goethe University Frankfurt, 60438 Frankfurt am Main, Germany

Correspondence: Andreas Kürten (kuerten@iau.uni-frankfurt.de)

Published: 19 November 2020

An error occurred in the paper “New particle formation from sulfuric acid and ammonia: nucleation and growth model based on thermodynamics derived from CLOUD measurements for a wide range of conditions” by Kürten (2019).

An index in one of the collision rates (Eq. S2f) of the code was wrong, which caused an imbalance between the production and loss rate for the clusters A_2B_1 and A_2B_2 . In the code representing the loss of cluster A_2B_1 due to collision with B_1 (term $K_{1,2} \cdot B_1$) the collision rate $K_{1,3}$ was used instead of $K_{1,2}$. This caused an imbalance since the loss rate for the cluster A_2B_1 from collision with B_1 (Eq. S2f) needs to match the production of cluster A_2B_2 from the collision of A_2B_1 with B_1 (see Eq. S2h). With the wrong collision rate in only one of the equations this is not the case anymore. As a result, for the same conditions, the error led to generally smaller nucleation rates because of the suppression of A_2B_1 cluster concentrations. The effect is more pronounced for larger ammonia concentrations.

After fixing this bug in the code, all calculations described in the article were repeated. The table and figures presented in the corrigendum are based on the corrected model. This applies also to Figs. S1 to S4 in the Supplement to this corrigendum.

The main differences between the original and the corrected version of the paper are highlighted in the following:

- The correct model yields a clear peak in the probability density function from the Monte Carlo method for the cluster A_2B_1 (Fig. 2). In the original article this was the case for the cluster A_2B_2 . The correct result

indicates that the cluster A_2B_1 is important for sulfuric acid–ammonia nucleation, which was also highlighted in a study by Hanson and Eisele (2002).

- The corrected results indicate a good agreement between modeled and measured CLOUD data (Fig. 3). However, the average error is somewhat larger compared with the results from the original article (factor of ~ 8 instead of ~ 4).
- The updated results for the optimization method indicate a stronger dependence on NH_3 (Fig. 4). This dependence is near to quadratic (instead of linear in the original article) for the warmer temperatures (248, 278 and 292 K). This leads to some overestimation in the modeled formation rates for these temperatures and high ammonia mixing ratios, especially at 278 K and NH_3 above 100 pptv. However, this region of the parameter space is not very well constrained by experimental data. On the other hand, the model predicts lower formation rates at 292 K under background ammonia mixing ratios (estimated value of ~ 4 pptv).
- Figure 5 indicates a close to quadratic dependence on NH_3 for 248 K and warmer temperatures. This is different to the original article with a linear dependence.
- No difference was found for the growth rates from the model between the original and the corrected version (Fig. 6 of the original paper).

- The model using the medians from the Monte Carlo simulation yields an overall error that is smaller than the one from the optimization method (Fig. S2). The average error between model and CLOUD data is a factor of 8 for the optimization method, whereas the Monte Carlo experiment yields a factor of 6. The data from the Monte Carlo simulation indicate additionally a weaker dependency on NH_3 . Here the dependency is rather linear than quadratic.
- The comparison between the Atmospheric Cluster Dynamics Code (ACDC) model (results shown in Kürten et al., 2016; for ACDC see McGrath et al., 2012) based on the thermodynamic data published in Ortega et al. (2012) and the present model using identical dH and dS values is shown in Fig. S3. In the original article the differences between these results were rather high, especially for warm temperatures (278 and 292 K). With the corrected model of the present study, this difference is small for all conditions where binary nucleation is negligible. However, while this can be taken as a verification of the SANTIAGO model, the Ortega et al. (2012) and the Hanson et al. (2017) data sets still do not represent the CLOUD data very well (see Figs. S3 and S4).

Regarding the conclusions, two statements from Sect. 5 of the original paper have to be reformulated. First, the average factor between modeled and measured CLOUD data is a factor of 8 for the optimization method (factor of 6 for the Monte Carlo method). In the original article a factor of 4 was reported. Second, the Ortega et al. (2012) thermodynamic data strongly overestimate the CLOUD data at warmer temperatures (248 K and above), which is consistent with the results from Kürten et al. (2016). Furthermore, the corrected version of SANTIAGO yields very similar results compared with the ACDC model (Fig. S3). In the original article SANTIAGO yielded much lower formation rates when using the Ortega et al. (2012) data set for the warm temperatures, and therefore the results were closer to the measured CLOUD data. This was attributed to the inclusion of the coagulation sink in SANTIAGO, which tends to lower the formation rates somewhat. However, these lower formation rates were mostly caused by the error in the code (see above). While the inclusion of the coagulation sink for formation rate calculations can still be important, its effect is therefore not as large as suggested in the original paper.

Table 1. dH and dS values from this study (^aoptimization method, ^bmedians from Monte Carlo simulation) and from the literature. dG values at 298 K. ^cData from Ortega et al. (2012). ^dData from Hanson et al. (2017). ^eData from Yu et al. (2018). ^fValue applies for cluster without involvement of water; with different amounts of water molecules this value varies between 11.52 and 12.59 kcal mol⁻¹. ^gValue applies for cluster without involvement of water; with different amounts of water molecules this value varies between 5.71 and 8.37 kcal mol⁻¹.

Reaction	$-dH$ (kcal mol ⁻¹)	$-dS$ (cal mol ⁻¹ K ⁻¹)	$-dG$ (kcal mol ⁻¹) at 298 K
$H_2SO_4 + NH_3 \rightleftharpoons (H_2SO_4)_1(NH_3)_1$	15.4 ^a , 12.3 ^b (16.00) ^c (15.0) ^d	28.2 ^a , 29.2 ^b (28.14) ^c (21.8) ^d	7.0 ^a , 3.6 ^b (7.61) ^c (8.5) ^d (7.77) ^e
$(H_2SO_4)_1(NH_3)_1 + H_2SO_4 \rightleftharpoons (H_2SO_4)_2(NH_3)_1$	27.6 ^a , 23.5 ^b (29.00) ^c (29.0) ^d	42.6 ^a , 42.8 ^b (42.90) ^c (52.0) ^d	14.9 ^a , 10.7 ^b (16.22) ^c (13.5) ^d (11.65) ^{e,f}
$(H_2SO_4)_2(NH_3)_1 + NH_3 \rightleftharpoons (H_2SO_4)_2(NH_3)_2$	18.5 ^a , 19.5 ^b (19.46) ^c (19.0) ^d	33.5 ^a , 33.5 ^b (33.41) ^c (26.8) ^d	8.5 ^a , 9.5 ^b (9.5) ^c (11.0) ^d (8.75) ^{e,g}
$(H_2SO_4)_2(NH_3)_1 + H_2SO_4 \rightleftharpoons (H_2SO_4)_3(NH_3)_1$	19.2 ^a , 24.6 ^b (21.06) ^c (26.0) ^d	37.1 ^a , 35.9 ^b (36.69) ^c (35.3) ^d	8.1 ^a , 13.9 ^b (10.13) ^c (12.5) ^d (7.08) ^e
$(H_2SO_4)_2(NH_3)_2 + H_2SO_4 \rightleftharpoons (H_2SO_4)_3(NH_3)_2$	29.4 ^a , 30.0 ^b (27.63) ^c (30.0) ^d	38.2 ^a , 38.0 ^b (38.74) ^c (36.9) ^d	18.0 ^a , 18.7 ^b (16.09) ^c (19.0) ^d (12.17) ^e
$(H_2SO_4)_3(NH_3)_2 + NH_3 \rightleftharpoons (H_2SO_4)_3(NH_3)_3$	26.8 ^a , 26.7 ^b (25.48) ^c (20.0) ^d	40.7 ^a , 40.8 ^b (41.04) ^c (28.5) ^d	14.7 ^a , 14.5 ^b (14.14) ^c (11.5) ^d (7.42) ^e
$(H_2SO_4)_3 + H_2SO_4 \rightleftharpoons (H_2SO_4)_4$	17.5 ^a , 22.2 ^b (16.78) ^c (23.0) ^d	27.3 ^a , 26.3 ^b (27.84) ^c (43.9) ^d	9.3 ^a , 14.4 ^b (8.48) ^c (9.9) ^d (n.a.) ^e
$(H_2SO_4)_3(NH_3)_1 + H_2SO_4 \rightleftharpoons (H_2SO_4)_4(NH_3)_1$	21.4 ^a , 21.0 ^b (21.34) ^c (24.5) ^d	43.5 ^a , 43.6 ^b (43.50) ^c (43.6) ^d	8.4 ^a , 8.0 ^b (8.38) ^c (11.5) ^d (4.16) ^e
$(H_2SO_4)_3(NH_3)_2 + H_2SO_4 \rightleftharpoons (H_2SO_4)_4(NH_3)_2$	23.5 ^a , 24.1 ^b (23.04) ^c (26.0) ^d	40.0 ^a , 40.1 ^b (40.15) ^c (36.9) ^d	11.6 ^a , 12.2 ^b (11.08) ^c (15.0) ^d (7.48) ^e
$(H_2SO_4)_3(NH_3)_3 + H_2SO_4 \rightleftharpoons (H_2SO_4)_4(NH_3)_3$	27.6 ^a , 29.2 ^b (27.60) ^c (30.0) ^d	38.1 ^a , 37.5 ^b (38.12) ^c (34.2) ^d	16.2 ^a , 18.0 ^b (15.36) ^c (19.8) ^d (12.34) ^e
$(H_2SO_4)_4(NH_3)_3 + NH_3 \rightleftharpoons (H_2SO_4)_4(NH_3)_4$	19.2 ^a , 19.4 ^b (19.18) ^c (21.0) ^d	28.7 ^a , 28.5 ^b (28.68) ^c (27.8) ^d	10.6 ^a , 10.9 ^b (10.63) ^c (12.7) ^d (11.34) ^e

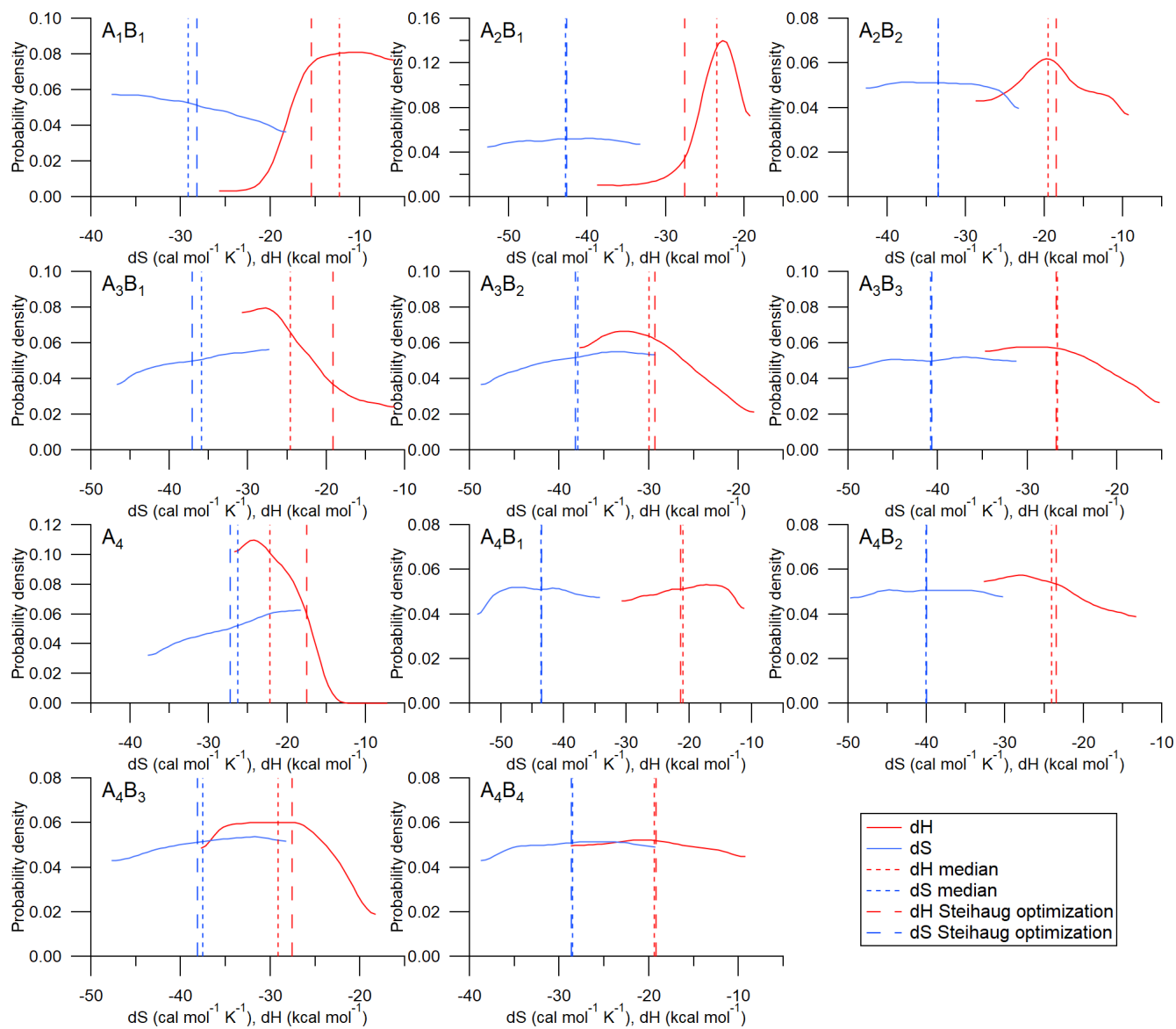


Figure 2. Probability density functions of dH and dS values for 11 clusters in the acid–base system (A_xB_y is a cluster of sulfuric acid and ammonia with x sulfuric acid molecules and y ammonia molecules). The vertical lines indicate the values from the optimization method (dashed lines) and the medians of the probability density functions (dotted lines).

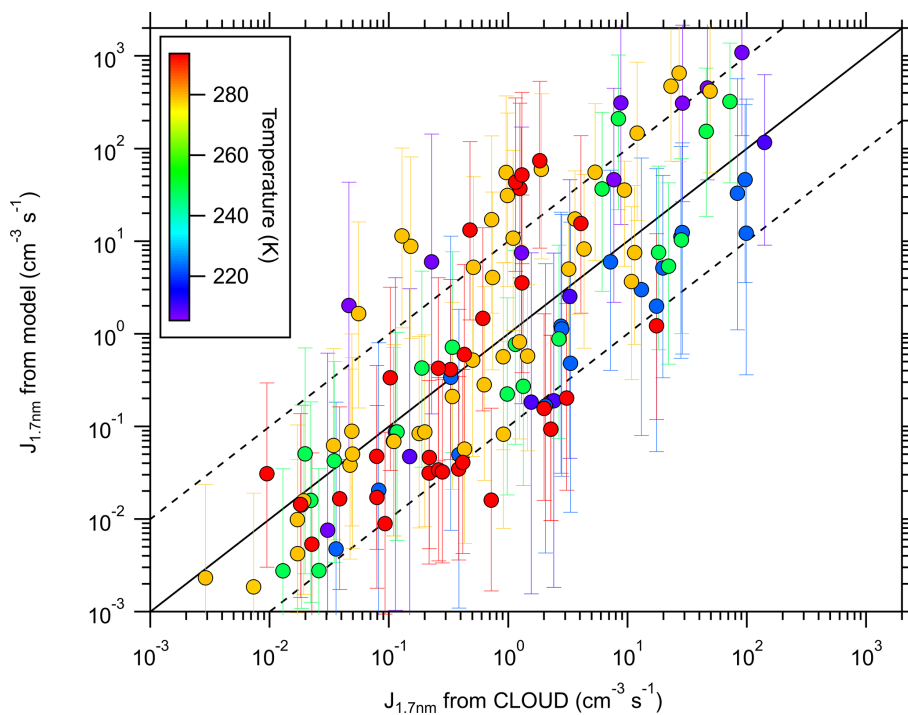


Figure 3. Calculated new particle formation (NPF) rates vs. measured NPF rates (from Kürten et al., 2016). The color code indicates the temperature (between 208 and 292 K). The calculated values are from the model using the thermodynamic data from Steihaug's optimization method. The solid line indicates the one-to-one correspondence, while the dashed lines indicate a deviation by a factor of 10 from the one-to-one line. The error bars include the uncertainty of the $[\text{H}_2\text{SO}_4]$ (factor of 2) and the $[\text{NH}_3]$ (see Kürten et al., 2016).

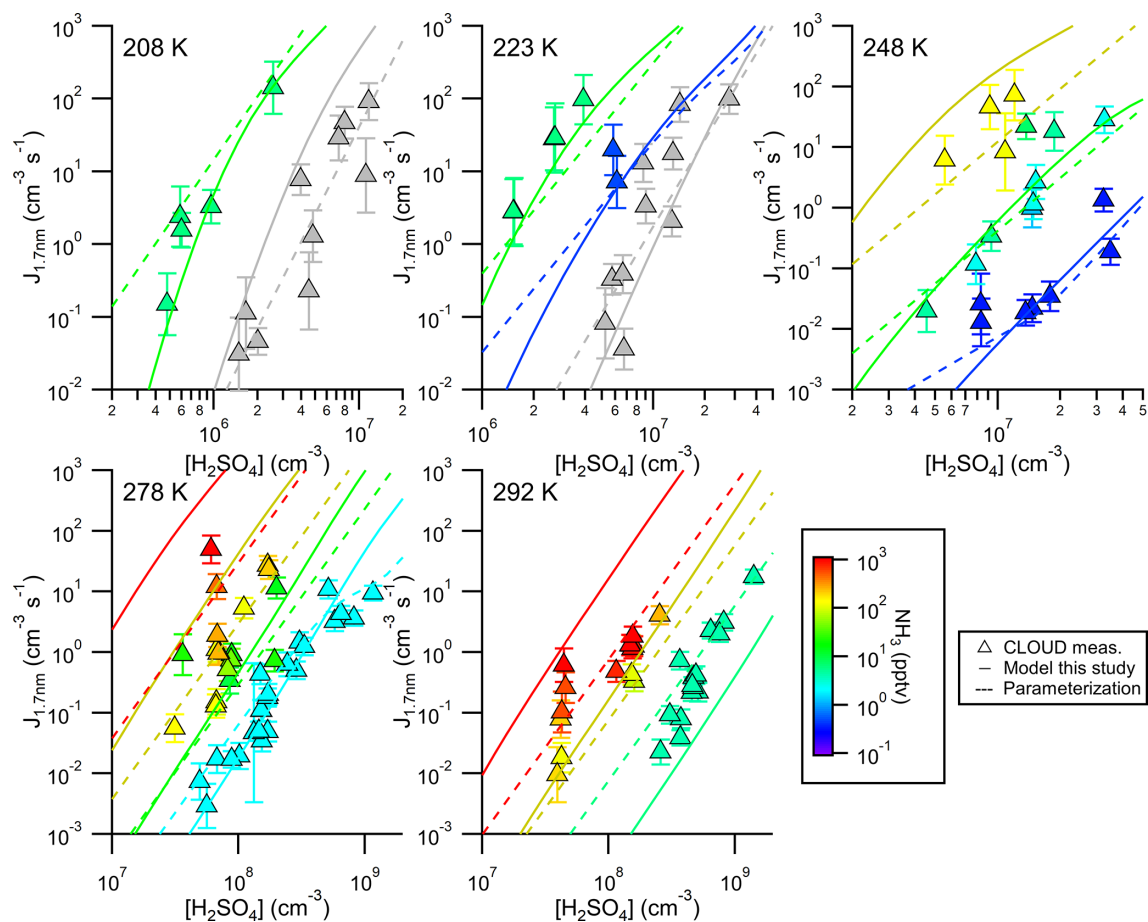


Figure 4. Comparison between simulated and measured new particle formation rates for five different temperatures. The color code indicates the ammonia mixing ratio (for the respective temperatures indicated in the figure panels and a pressure of 1 bar); the grey symbols indicate pure binary conditions. The model (solid lines) uses thermodynamic data from the optimization scheme according to Steihaug (1983, Sect. 2.4). The average ratio for the deviation is ~ 8 . In comparison, the results from the parameterization are also shown (dashed lines; Gordon et al., 2017).

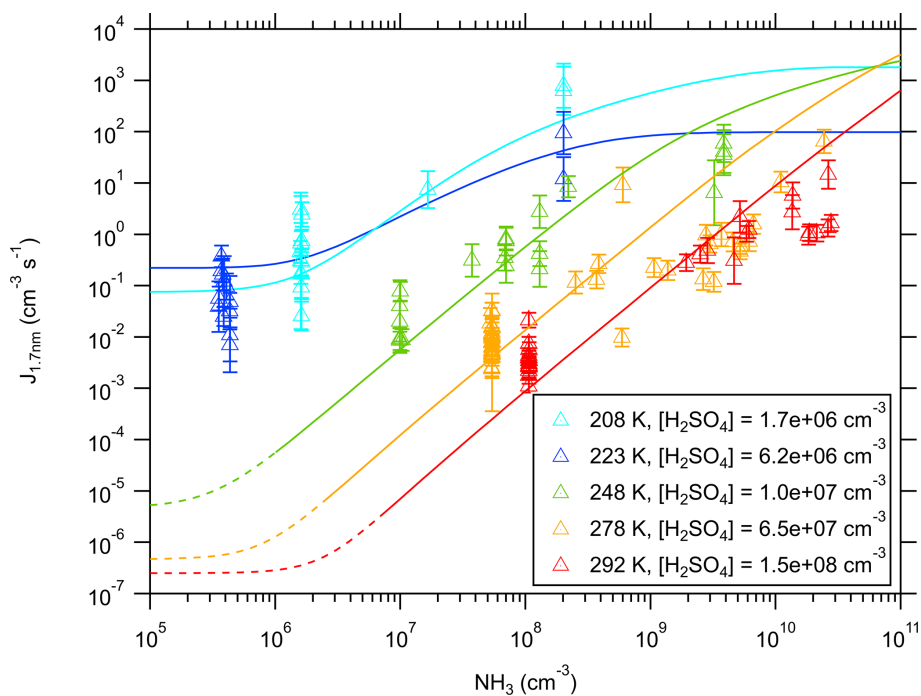


Figure 5. New particle formation rates as a function of the ammonia concentration. The triangles show the neutral formation rates from the CLOUD experiment normalized to the indicated sulfuric acid concentration for five different temperatures (Kürten et al., 2016). The lines show calculated NPF rates from the model using the thermodynamic data from the optimization method (Table 1). The dashed sections (for 248, 278, and 292 K) indicate regions of the parameter space where the model does not give accurate results, as the true binary rates are expected to be lower (Ehrhart et al., 2016).

References

- Ehrhart, S., Ickes, L., Almeida, J., Amorim, A., Barmet, P., Bianchi, F., Dommen, J., Dunne, E. M., Duplissy, J., Franchin, A., Kangasluoma, J., Kirkby, J., Kürten, A., Kupc, A., Lehtipalo, K., Nieminen, T., Riccobono, F., Rondo, L., Schobesberger, S., Steiner, G., Tomé, A., Wimmer, D., Baltensperger, U., Wagner, P. E., and Curtius, J.: Comparison of the SAWNUC model with CLOUD measurements of sulphuric acid-water nucleation, *J. Geophys. Res.-Atmos.*, 121, 12401–12414, <https://doi.org/10.1002/2015JD023723>, 2016.
- Gordon, H., Kirkby, J., Baltensperger, U., Bianchi, F., Breitenlechner, M., Curtius, J., Dias, A., Dommen, J., Donahue, N. M., Dunne, E. M., Duplissy, J., Ehrhart, S., Flagan, R. C., Frege, C., Fuchs, C., Hansel, A., Hoyle, C. R., Kulmala, M., Kürten, A., Lehtipalo, K., Makhmutov, V., Molteni, U., Rissanen, M. P., Stozhkov, Y., Tröstl, J., Tsagkogeorgas, G., Wagner, R., Williamson, C., Wimmer, D., Winkler, P. M., Yan, C., and Carslaw, K. S.: Causes and importance of new particle formation in the present-day and preindustrial atmospheres, *J. Geophys. Res.-Atmos.*, 122, 8739–8760, <https://doi.org/10.1002/2017JD026844>, 2017.
- Hanson, D. R. and Eisele, F. L.: Measurement of prenucleation molecular clusters in the NH_3 , H_2SO_4 , H_2O system, *J. Geophys. Res.-Atmos.*, 107, 4158, <https://doi.org/10.1029/2001JD001100>, 2002.
- Hanson, D. R., Bier, I., Panta, B., Jen, C. N., and McMurry, P. H.: Computational Fluid Dynamics Studies of a Flow Reactor: Free Energies of Clusters of Sulfuric Acid with NH_3 or Dimethyl Amine, *J. Phys. Chem. A*, 121, 3976–3990, <https://doi.org/10.1021/acs.jpca.7b00252>, 2017.
- Kürten, A., Bianchi, F., Almeida, J., Kupiainen-Määttä, O., Dunne, E. M., Duplissy, J., Williamson, C., Barmet, P., Breitenlechner, M., Dommen, J., Donahue, N. M., Flagan, R. C., Franchin, A., Gordon, H., Hakala, J., Hansel, A., Heinritzi, M., Ickes, L., Jokinen, T., Kangasluoma, J., Kim, J., Kirkby, J., Kupc, A., Lehtipalo, K., Leiminger, M., Makhmutov, V., Onnela, A., Ortega, I. K., Petäjä, T., Praplan, A. P., Riccobono, F., Rissanen, M. P., Rondo, L., Schnitzhofer, R., Schobesberger, S., Smith, J. N., Steiner, G., Stozhkov, Y., Tomé, A., Tröstl, J., Tsagkogeorgas, G., Wagner, P. E., Wimmer, D., Ye, P., Baltensperger, U., Carslaw, K., Kulmala, M., and Curtius, J.: Experimental particle formation rates spanning tropospheric sulfuric acid and ammonia abundances, ion production rates and temperatures, *J. Geophys. Res.-Atmos.*, 121, 12377–12400, <https://doi.org/10.1002/2015JD023908>, 2016.
- McGrath, M. J., Olenius, T., Ortega, I. K., Loukonen, V., Paasonen, P., Kurtén, T., Kulmala, M., and Vehkamäki, H.: Atmospheric Cluster Dynamics Code: a flexible method for solution of the birth-death equations, *Atmos. Chem. Phys.*, 12, 2345–2355, <https://doi.org/10.5194/acp-12-2345-2012>, 2012.
- Ortega, I. K., Kupiainen, O., Kurtén, T., Olenius, T., Wilkman, O., McGrath, M. J., Loukonen, V., and Vehkamäki, H.: From quantum chemical formation free energies to evaporation rates, *Atmos. Chem. Phys.*, 12, 225–235, <https://doi.org/10.5194/acp-12-225-2012>, 2012.
- Steihaug, T.: The Conjugate Gradient Method and Trust Regions in Large Scale Optimization, Society for Industrial and Applied Mathematics, 20, 626–637, 1983.
- Yu, F., Nadykto, A. B., Herb, J., Luo, G., Nazarenko, K. M., and Uvarova, L. A.: H_2SO_4 - H_2O - NH_3 ternary ion-mediated nucleation (TIMN): kinetic-based model and comparison with CLOUD measurements, *Atmos. Chem. Phys.*, 18, 17451–17474, <https://doi.org/10.5194/acp-18-17451-2018>, 2018.